Published in final edited form as:
Neurobiol Dis. 2012 April ; 46(1): 59–68. doi:10.1016/j.nbd.2011.12.044.

Intraspinal transplantation of neurogenin-expressing stem cells generates spinal cord neural progenitors

J. Simon Lunn[a], **Crystal Pacut**[a], **Emily Stern**[a], **Stacey A. Sakowski**[a], **J. Matthew Velkey**[b,1], **Sue O'Shea**[b], and **Eva Feldman**[a]

[a]Department of Neurology, University of Michigan, Ann Arbor, MI, 48109

[b]Department of Cell and Developmental Biology, University of Michigan, Ann Arbor, MI, 48109

Abstract

Embryonic stem (ES) cells and their derivatives are an important resource for developing novel cellular therapies for disease. Controlling proliferation and lineage selection, however, are essential to circumvent the possibility of tumor formation and facilitate the safe translation of ES-based therapies to man. Expression of appropriate transcription factors is one approach to direct the differentiation of ES cells towards a specific lineage and stop proliferation. Neural differentiation can be initiated in ES cells by expression of Neurogenin1 (Ngn1). In this study we investigate the effects of controlled Ngn1 expression on mouse ES (mES) cell differentiation i*n vitro* and following grafting into the rat spinal cord. *In vitro*, Ngn1 expression in mES cells leads to rapid and specific neural differentiation, and a concurrent decrease in proliferation. Similarly transplantation of Ngn1-expressing mES cells into the spinal cord lead to *in situ* differentiation and spinal precursor formation. These data demonstrate that Ngn1 expression in mES cells is sufficient promote neural differentiation and inhibit proliferation, thus establishing an approach to safely graft ES cells into the spinal cord.

Keywords

Embryonic stem cells; Neurogenin1; Neural specification; Spinal cord

INTRODUCTION

Embryonic stem (ES) cells have the potential to provide both cellular replacement and environmental enrichment, and are gaining interest as treatments for spinal cord injury and neurodegenerative disorders including amyotrophic lateral sclerosis (ALS), spinal muscular atrophy (SMA), stroke, and multiple sclerosis (Lunn et al., 2011; Payne et al., 2011; Sobani et al., 2010). The overall safety of ES cell transplantation, however, poses a significant limitation on the potential use of these novel stem cell therapies (Drukker, 2006; Hentze et al., 2009). Developing strategies to overcome adverse events including uncontrolled

Corresponding author: Eva L. Feldman, MD, PhD, 109 Zina Pitcher Place, 5017 AATBSRB, Ann Arbor, MI 48109, Phone: 734-763-7274, Fax: 734-763-7275, efeldman@umich.edu.
[1]Current address: Department of Cell Biology, Duke University, Durham, NC, 27708

proliferation and incorrect lineage differentiation is important for the clinical translation of ES cell technology (Goldring et al., 2011).

There are numerous therapeutic approaches that utilize neural progenitor cells (Lunn et al., 2011; Nishimoto et al., 2011; Yan et al., 2007). These cells, however, have limited availability and restricted differentiation potential based on the cells' origin or specific culture conditions. ES cells, on the other hand, are widely available and may be stimulated to become neural progenitors. In addition, ES cells have a broader differentiation potential, and thus may provide a larger range of neuronal subtypes. In order to harness the potential therapeutic advantages of ES cells, unregulated proliferation and the development of tissue-inappropriate lineages needs to be controlled, and a safe approach to incorporate these cells into the central nervous system must be developed (Chung et al., 2006; Jung et al., 2007; Kiuru et al., 2009).

One way to both minimize unregulated proliferation and control lineage specification is through expression of selective pro-neural regulatory factors during ES cell implantation. These factors drive the differentiation of developing ES cells towards desired lineages and in turn check excessive proliferation. Neurogenin 1 (Ngn1), a neurogenic basic helix loop helix (bHLH) transcription factor, is sufficient to drive neural differentiation and inhibit gliogenesis (Farah et al., 2000; Kim et al., 2008; Morrison, 2001; Reyes et al., 2008). Ngn1 is expressed in the neural tube during development where it is a neural specification factor (Chesnutt et al., 2004; Nakada et al., 2004); therefore, overexpression of Ngn1 may initiate the differentiation of ES cells to promote subsequent patterning towards a spinal neural identity.

Ngn1-expressing mES cells under the control of a tet-on promoter allow the controllable induction of Ngn1 (designated N7 cells). After stimulation and expression of Ngn1, N7 cells differentiate to neural lineages and are electrophysiologically active within 4 days of culture (Reyes et al., 2008; Tong et al., 2010). When cultured with BDNF and GDNF, 75% of the cells achieve a glutamatergic phenotype. Four weeks after engraftment into the inner ear of guinea pig, the majority of N7 cells differentiate into neural lineages with limited GFAP-positive cells and approximately 20–30% ES cells remaining (Reyes et al., 2008). No tumor formation was evident (Reyes et al., 2008).

In the current study, we examine the differentiation and proliferation profiles of mouse N7 cells without additional neurotropic support. Specifically, we characterize the effect of Ngn1 expression on the ability of the cells to proliferate, and differentiate *in vitro*. Furthermore, we optimize an approach to utilize Ngn1 expression to prevent uncontrolled proliferation and safely utilize mES cells for rat intraspinal transplantation. Finally, we assess viability of N7 to respond to the microenvironment and and demonstrate that the cells are capable of differentiating into various spinal progenitors cell types after only 2 weeks *in situ*. Overall, controlled Ngn1 expression in ES cells provides a means to circumvent unregulated proliferation and incorrect lineage selection which limits ES cell therapeutic application, and establishes an approach to transplant ES cells into the spinal cord to recapitulate cell types that may be lost in injury and disease.

MATERIALS & METHODS

Cell Culture

The parental Ainv15 cell line contains a reverse tet transactivator upstream of the constitutively active ROSA26 locus that has a puromycin selectable cassette (Kim et al., 1997). To establish Ngn1-inducible mES cells, (N7 cells) the Ainv15 cells were modified to express Ngn1 by integrating a plasmid containing the Ngn1 cDNA and an ATG start codon

into the Anvi15 cell genome upstream of the tet operon. Downstream of the integration site, a truncated neomycin resistance cassette was placed into the line making it G418 selectable. N7 cells can be selected by growing in the presence of both puromycin and G418 (velkey, 2005).

N7 cells are cultured on 0.1% gelatin-coated substrates in complete growth media. Complete growth media contains high glucose DMEM (Gibco) supplemented with 10% ES-tested fetal bovine serum (FBS; University of Michigan Transgenic Core) and 1000 units/ml human recombinant Leukemia inhibitory factor (LIF, Chemicon). To maintain cells in an undifferentiated state, N7 cells are grown in media plus 350 μg/ml G418 and 1.5 μg/ml puromycin (Kelloff and Sigman). For neural differentiation, N7 cells were plated at 1.0×10^5 cell/cm^2 on gelatin-coated 6-well dishes or on gelatin-coated glass coverslips in 24-well plates. N7 cells were placed in defined differentiation media consisting of 80% DMEM/F12 (Gibco) and 20% Neurobasal media (Gibco) augmented with 10 μg/ml MEM pyruvate (Invitrogen), 8 μg/ml N2 supplement (Invitrogen) and 4 μg/ml retinoic acid (RA)-free B27 supplement (Invitrogen). To induce Ngn1 expression, differentiation media was supplemented with 1 μg/ml Doxycyclin (Dox) (Kelloff and Sigman). For motor neuron differentiation, N7 cells were trypsinized (Gibco) from the plates and placed in ADFNK media (45% Advanced DMEM/F12 45% Neurobasal media, 10% KOSR (Gibco), 0.1mM 2-mercaptoethanol) in non-adhesive petri dishes to develop embryoid bodies (EBs). After the formation of EBs, we followed protocols treating EBs with retinoic acid (RA) and sonic hedgehog (shh) over one week (Wichterle and Peljto, 2008).

Animal studies

All rat (Sprague Dawley, Taconic NY) surgeries, recovery, animal behavior and monitoring to end-stage disease were conducted with appropriate institutional oversight and University Committee on Use and Care of Animals approval. Animals were pretreated with Dox in their drinking water at levels that penetrate the blood brain barrier for 3 days (d) prior to surgery to equilibrate the tissue. Briefly, drinking water containing 2 g/l Dox and 5% sucrose was provided to the animals 3 d prior to surgery and continued for 7 d. Water was protected from light and changed every 2 d. Animals were observed for signs of dehydration and given saline as needed (Cawthorne et al., 2007). After Dox equilibration, the animals underwent a laminectomy to expose the spinal cord at L2–L5 for subsequent N7 cell or media control injections.

One h prior to injection, the N7 cells were collected and adjusted to a final concentration of 5,000 cells per 1 μl in defined differentiation media with Dox (1 μg/ml). Animals were anesthetized by isoflurane induction and shaved prior to surgery. The animals were stabilized using the Cunningham spinal adaptor (Stoelting, IL) and the L2–L5 spinal cord was exposed by removing the spinal processes using a surgical drill (ConMed Linvatec, FL). Five unilateral injections of 5,000 cells were delivered using a Hamilton syringe connected to a 32 gauge needle using a Kopf mircoinjection unit (David Kopf Instruments, CA). The center of the injection was targeted into the ventral gray matter. The rostrocaudal distance between individual injections was approximately 5 mm. Cell culture media of equal volume served as a control. After implantation, the incision was closed in two layers. Transplanted animals were immunosuppressed with 1 mg/kg/d Prograf (Tacrolimus capsules, Fujisawa Healthcare) starting 3 d prior to transplantation and maintained throughout the experiment (Hefferan et al., 2011). To assess locomotor function, rats were assessed using the Basso, Beattie and Bresnahan (BBB) score, and an open-field 21-point scale that tests hindlimb movement, stepping and weight bearing. Daily weights and weekly BBB scores were assessed throughout the animals' lifetime. The experiment was terminated following either a 10% loss of body weight and loss of hindlimb function (BBB locomotion score of 0), or if 2

wk post-surgery had passed. The animals were sacrificed by deep anesthesia (pentobarbital 40 mg/kg and phenytoin 25 mg/kg by intraperitoneal (IP) injection) (Xu et al., 2006).

Immunostaining

Immunohistochemistry (IHC) was carried out by standard protocols as previously described (Lunn et al., 2009). Briefly, N7 cells were grown on gelatin-coated glass coverslips in 24-well plates and fixed with 2% PFA for 10 min. Spinal cord tissues were fixed in 2% PFA and were cryoprotected in 30% sucrose prior to cryosectioning (20 micron). Fixed cells or spinal cord sections were permeabilized with 0.1% Triton/PBS and blocked in 5% normal donkey serum/0.1% Triton/PBS. Sections or cells were incubated with the following antibodies were incubated overnight at 4°C: Ngn1 (Abcam, 1:500); Sox2 (Thermo, 1:500); Sox3 (gift M. Klymkowsky, University of Colarado); Tuj1 (Neuromics, 1:1000); Foxa2 (Millipore, 1:250); Brachyury (Santa Cruz, 1:250); GluR1 (Abcam, 1:500); Oct3/4 (Santa Cruz, 1:500); Nestin (Neuromics, 1:500); Islet1/2 (Developmental Studies Hybridoma Bank (DHB), 1:50); Olig2 (Millipore, 1:500); Pax3 (DHB, 1:500); Pax6 (DHB, 1:500); Nkx6.1 (DHB, 1:500); Nkx2.2 (DHB, 1:500). Cells and sections were then incubated in appropriate Cy3, Cy5, or FITC-conjugated secondary antibodies (Jackson ImmunoResearch, Westgrove, PA) followed by mounting on glass slides using ProLong Gold with DAPI (MolecularProbes, Invitrogen, Carlsbad, CA). Alternatively, some spinal cord slices were stained with hemotoxylin and eosin (H&E) using standard protocols. Images were collected using an Olympus BX-51 microscope.

Proliferation

To measure proliferation, cells were grown as above and incubated with 10 μM 5-ethynyl-2'-deoxyuridine (EdU) for 1 h prior to fixation and processed following the manufacturers' protocol for the Click-It EdU kit (Invitrogen, Carlsbad, CA). EdU incorporation was measured by fluorescent imaging using an Olympus BX-51 microscope. Secondly, a FACS analysis between the N7 cell treatment groups was carried out. The cells were grown with or without Dox for 3 d, while a control flask kept in ES cell growth conditions was also treated. The cells were trypsinized and adjusted to 1×10^6 cells with 0.5 ml PBS. Cold 100% ethanol (0.5ml) was added drop-wise and the cells were vortexed and incubated on ice for 20 min. The cells were centrifuged and ethanol was removed. Propidium iodide (PI; 0.5ml) mix was added to a final concentration of 50 μg/ml PI (Sigma) and 100 μg/ml RNAse Type I-A (Sigma) in PBS. The cells were mixed well and incubated for 20 min. Samples were run on FacsCaliber machine (University of Michigan Flow Cytometry Core) and data was analyzed using ModFitLT.

Western Blotting

Western blotting was performed as previously described (Lunn et al., 2009). Briefly. N7 cell lysates were prepared by scraping cells in modified RIPA buffer (20 mM Tris, pH 7.4, 150 mM NaCl, 1 mM EDTA, 0.1% SDS, 1 mM Na deoxycholate, 1% Triton X-100, 0.1 trypsin units/L aprotinin, 10 mg/mL leupeptin, and 50 mg/mL PMSF). Equal amounts of protein were loaded in each lane of a polyacrylamide gel, with gel percentages (either 7.5%, 12.5%, or 15%) dependent on the size of the protein of interest. Protein gels were then transferred onto PVDF membranes and incubated with primary antibody overnight at 4°C followed by appropriate horseradish peroxidase-conjugated secondary antibodies (Santa Cruz Biotechnology, SantaCruz, CA) for 1 hr at room temperature. The following antibodies were utilized: Oct3/4 (1:200), Sox2 (1:500), and Tuj1 (1:2000). Antibody binding was developed with LumiGLO Reagent and Peroxide (Cell Signaling) and exposed to Kodak BioMax XAR film (Sigma). Each experimental paradigm was tested on 3 separate occasions using different cultures or tissue samples. Membranes were re-probed for GAPDH (Santa Cruz 1:2000) to confirm equal protein loading.

RNA isolation and quantitative real-time PCR (QPCR)

Total RNA was extracted from N7 cells or EBs using an RNeasy Kit (Qiagen, Valencia, CA, USA) according to the manufacturer's instructions. Reverse transcription was performed using the iScript cDNA Synthesis Kit (Bio-Rad). QPCR reactions were carried out in 96-well 0.2 ml PCR plates sealed with iCycler Optical Sealing tapes (Bio-Rad). The QPCR amplification profile was as follows: 95°C for 5 min; 40 cycles of denaturation at 95°C for 30 s, annealing at 58°C for 1 min, extension at 72°C for 30 s; and a final phase of 72°C for 5 min. The fluorescence threshold Ct value was calculated by the iCycler iQ system software and the levels were first normalized to the endogenous reference actin (ΔCt), followed by relation to the control (ΔΔCt) and expressed as 2-ΔΔCT. QPCR product levels were expressed as mean ± SEM and a two-sample equal variance t-test was performed (n=3 replicates over 3 independent experiments).

RESULTS

In vitro induction of neurogenesis by Ngn1

N7 cells were grown either in the presence (+Dox) or absence (−Dox) of Dox for 3 d and stained using a collection of stem, neural and lineage markers. N7 cells were co-labeled with DAPI to ensure that the cells were at similar densities and to highlight any negative cells. Representative images are shown in Figure 1. Prior to stimulation, N7 cells expressed the embryonic stem cell markers Sox2 (Figure. 1 B) and Oct3/4 (data not shown). Cells growing in basal ES conditions at d 0, did not express the neural genes Ngn1, Sox3, or TuJ1 (Figure. 1 A,C,D), nor the mesodermal or endodermal markers Brachyury or Foxa2 (Figure. 1 E,F). After 3 d of growth -Dox, there was maintained expression of the stem marker Sox2 (Figure. 1 I) and also observed low levels of Sox3 expression (Figure. 1 J). After 3 d of growth +Dox, there was an increase in Ngn1 expression (Figure .1 O) and a reduction in Sox2 expression (Figure. 1 P). There was also an increase in the pan-neural marker Sox3 (Figure. 1 Q) and in the early neuronal markerTuj1 (Figure. 1 R). Neither condition promoted expression of Brachyury or Foxa2 (Figure. 1 L,M,S,T). N7 cells grown +Dox express GluR2, a marker of a more mature neural phenotype (Figure. 1 U); however, no GFAP staining was observed (data not shown). Together these data demonstrate that Ngn1 promotes neural differentiation of mES cells.

To confirm the IHC results following Dox stimulation, we performed western blot and QPCR analysis. We first assessed expression of the stem cell markers Oct3/4 and Sox2, and the neuronal marker Tuj1 by western blotting. Western analysis demonstrates equal levels of the stem marker Oct3/4 after 24 h of +/− Dox treatment (Figure. 2 A,B). At 48 h, there is less Oct3/4 in the +Dox condition, and this decreasing trend continues through 72 h. Sox2 demonstrates a similar reduction, as expression declined after 24 h +Dox (Figure. 2 A,B). Western blot analysis showed TuJ1 expression within 48 h of +Dox (Figure. 2 A,C). Next, QPCR demonstrated that Dox induction of Ngn1 was very robust, with a 400-fold increase in Ngn1 within 24 h of Dox treatment (Figure. 2 D). More so, the stem cell marker Nanog exhibits striking decreased expression which is lost altogether within 24 h +Dox (Figure. 2 E). QPCR for the neural marker Nestin demonstrates an increase in expression by 24 h that was statically significant by 48 and 72 h (Figure. 2 F). There was a slight increase in Nestin in N7 cells grown −Dox by 3 d, likely due to culture in differentiation media (Figure. 2 F). We did not observe an increase of either Brachyury or Foxa2 by QPCR over the first 3 d (data not shown). Together, analyses by western blotting and QPCR confirm the robust expression of Ngn1 in response to Dox treatment. Furthermore, expression of Ngn1 leads to a rapid loss of stem cell identity and differentiation towards a neural lineage.

Proliferation

Given that cell overgrowth poses a potential hurdle for transplantation applications, we next assessed the effect of the Dox treatment on cell proliferation. Cells were differentiated for 3 d +/−Dox, after which cells were treated with EdU for 1 h and processed. EdU analysis demonstrated that approximately 40% of the cells were proliferating in the absence of Dox (Figure. 2 G). Dox exposure resulted in a significant decrease to 20% proliferating cells (Figure. 2 G). To further examine the change in proliferation, we carried out cell cycle analysis of PI-stained N7 cells using FACS analysis. Undifferentiated N7 cells and N7 cells −Dox displayed similar results. In each growth environment, approximately 42.5% of cells were in G0/G1 with 50% and 7.5% in S and G2/M, respectively (Figure. 2 H). On the other hand, N7 +Dox exhibited an increase to 76% of cells in G0/G1, with a reduction to 19% in S and 4% in G2/M (Figure. 2 H). When cell death was quantified by FACS, N7 cells +Dox exhibited a 10% increase compared to N7 cells −Dox (Figure. 2 H). Overall these data demonstrate that expression of Ngn1 leads to a rapid exit from cycle.

In vitro differentiation

To determine if the induction of Ngn1 altered the ability of N7 cells to respond to differentiation cues, we next examined the response to patterning using motor neuron differentiation protocols. After 3 d +/− Dox, N7 cells were grown as EBs and cultured in one of two environments: in patterning conditions for motor neuron differentiation (+RA/Shh), or maintained in differentiation media (−RA/Shh). Ngn1 expression is maintained in all cells exposed to Dox, even after EB formation (Figure. 3 A). EBs +RA/Shh −Dox also expressed Ngn1 after 7 d (Figure. 3 A). Expression of the stem cell marker Oct 3/4 was only present in −RA/Shh −Dox condition (Figure. 4 A). The combination of +RA/Shh +Dox showed the highest levels of Nestin expression (Figure. 3B). Only −RA/Shh −Dox exhibited no Nestin staining. While all groups showed expression of vGlut, the highest levels were in the +RA/Shh +Dox group (Figure. 3 D).

To quantify the differences we observed between patterning groups we performed QPCR on all four groups of EBs, +/− RA/Shh and +/− Dox. QPCR on the EBs for the stem cell marker Sox2 showed a reduction in all groups when compared to −RA/shh −Dox (basal EB), with the greatest decrease being in the +RA/Shh +Dox group (Figure. 4 B). When we quantified neural differentiation by examining the expression of Nestin, we observed an increase in all groups when compared to the basal EB group (Figure. 4 C). Both groups that included +RA/Shh exhibited the highest Nestin staining, likely a response to the pro-neural culture conditions. QPCR quantification for GluR2 demonstrated a large, 40-fold increase in expression in the +RA/Shh +Dox culture condition indicative of a higher number of mature neurons. When we assessed the expression of Islet 1/2 as a marker of motor neuron differentiation, we observed expression of Islet 1/2 in both +RA/Shh groups, with no Islet 1/2 expression in −RA/Shh groups (Figure. 4 D). We did not observe any difference in GFAP by IHC (data not shown), and expression of GFAP by QPCR was not altered +/− RA/Shh (Figure. 4 D). We also did not observe any staining for Foxa2 or Brachyury by IHC (data not show), which was confirmed by QPCR (Figure. 4 G,H).

Next we looked at Olig2, which is a marker of presumptive motor neurons, and Islet 1/2, which specifically labels motor neurons in the spinal cord, because exposure to RA/shh has been shown to promote motor neuron differentiation. Neither Olig2 nor Islet 1/2 were expressed in EBs grown −RA/Shh (Figure. 3 D, E). When the number of positive cells per EB was calculated, there were equal proportions of Olig2-positive cells and Olig2/Islet1/2 co-labeled cells +/− Dox treatment (Figure. 3 F). There was, however, a significant 6% increase in the number of cells that were singularly labeled with Islet 1/2 in the +Dox treatment group. Together, these data confirm that N7 cells are capable of responding to

patterning factors after prolonged Ngn1 expression and give rise to mature neurons. Furthermore, Ngn1 expression does not perturb the ability of N7 cells to be patterned toward a motor neuron phenotype.

In situ differentiation of N7 cells

Next, we established the optimal conditions for successful intraspinal injection of N7 cells, by assessing the graft safety which includes graft cell survival, cellular growth and cellular differentiation. Animals received Dox for 3 d prior to laminectomy and grafting to equilibrate systemic Dox levels for induction of N7 differentiation *in situ*. Seven d post-laminectomy, animals had a poor recovery from surgery. They exhibited significant weight loss and non-improving low BBB locomotor scores. When we examined the lumbar spinal cord, the N7 cells had overgrown the graft area and formed large tumors (Figure.5 A). The majority of the graft stained positive for Nestin and Oct 3/4 (data not shown). This approach was insufficient to stop proliferation and induce neural induction without causing damage to the spinal cord.

In order to reduce the cellular overgrowth, we pretreated the N7 mES cells and the animals with Dox for 3 d prior to grafting. After the primed N7 mES cells were grafted into the spinal cord the animals had better recovering BBB scores. The animals were harvested after 2 wk for investigation into the differentiation and developmental stages of the grafts. Initial H&E staining demonstrated that the cellular grafts could be identified either as a dorsal bolus of cells or a graft area that traced the injection tract (Figure. 5 B,C). After pretreating the N7 cells with Dox, we did not observe any tumor formation. The area of graft cells was stained with DAPI and was clearly visible as a compacted mass of cells. In order to ensure that we could use DAPI to identify the graft area, we determined the expression of Ngn1 in the spinal cord (Figure. 4 E). Ngn1 was not expressed in the contralateral side of the spinal cord and was only observed in the area of the graft. From then on, in order to assess the fate of N7 cells in the spinal cord, we only assessed cells within the area of the cell bolus. While this excluded any cells that may have migrated from the injection site, it ensures we were predominantly investigating the fate of the injected N7 cells.

To assess the number of N7 cells that continued to proliferate or maintained a stem phenotype, the spinal cords were stained for Ki67 and Oct3/4, respectively (Figure 5. C,D). We quantified the graft area in 3 individual images from the L2–L5 injection region representing over 1000 total cells counted. Only 7% of the graft stained for Oct3/4, and 12% were Ki67-positive cells. Expression of the alternative stem cell marker, Sox2, was observed in some cells in the contralateral side of the spinal cord, however, there were no cells within the graft area that expressed Sox2 (Figure. 5 F). Overall these results demonstrated that Dox primed N7 cells can safely be incorporated into the spinal cord without leading to tumor formation.

In situ patterning of N7 cells in the spinal cord

During normal development of the spinal cord, neural progenitor cells are exposed to opposing gradients of signaling factors that result in a dorsoventral pattern of domains that may be identified by their expression of specific transcription factors (illustrated in Figure.6 G). We therefore examined the early fate of the N7 cells differentiating in the spinal cord. The dorsal marker Pax3 positively stained approximately 30% of the graft area (Figure. 6 A,G), whereas the ventral marker Pax6 stained 3% of the graft area (Figure. 6 D). The sub-ventral markers Nkx6.1 and Nkx2.2 labeled 16% and 26% of the graft area, respectively (Figure. 6 B,E). Olig2 stained 26% of the grafted cells (Figure. 6 E). We lastly stained the cord for the pan-neural marker Sox3 (Figure. 6 C). While there were only a few Sox3-positive cells, they were also present on the contralateral side of the spinal cord (Figure. 6

C'). These data demonstrate that after grafting into the spinal cord, neural progenitors derived from mES cells respond to endogenous factors and recapitulate many of the neuronal sub-types of the spinal cord.

DISCUSSION

Many neurological disorders may benefit from stem cell-based therapies which have the potential to provide both cellular replacement and/or environmental enrichment. Current studies primarily utilize neural progenitors as the source of cells used in transplants, however, these cells have limited differentiation potential and availability. ES cells remain one of the greatest untapped resources available for cellular therapies with greater availability and unrestricted differentiation potential. However, transplantation of ES cells have been met with somewhat less enthusiasm, due in part to the concern of tumor formation and uncontrolled differentiation leading to ectopic differentiation of cells from undesired germ layers. To overcome these caveats and enhance the therapeutic potential of ES cells, we must specifically differentiate them into the type of cells needed to support the diseased tissue and prevent excessive proliferation. The ability to replicate the developmental processes that first establish specific cell types is necessary to differentiate the ES cells into the lineages needed to provide therapeutic effects.

Ngn1 is a member of a family of neurogenic factors that is required and sufficient for neural differentation (Kim et al., 2004; Nakada et al., 2004; Quinones et al., 2010). Ngn1 is expressed throughout the primitive neural tube, and later is restricted to a ventral domain of the spinal cord (Quinones et al., 2010). We hypothesized that we could generate neural progenitors, by expressing Ngn1, after which these cells may continue to further differentiate *in situ* into appropriate cell types for the spinal cord (Figure. 6 G). In the current study, we have elucidated the effects of Ngn1 expression on mES cells *in vitro*, and subsequently demonstrated that Ngn1 expression is sufficient to drive neural differentiation within of the spinal cord.

We first investigated the efficiency of Ngn1 under the inducible tet-on promoter which drives neural delineation in N7 cells. Consistent with previous observations (Reyes et al., 2008; velkey, 2005) Dox induced expression of Ngn1 very rapidly increased within 24 h of exposure (Figure. 2 D). Within 3 d there was a 400-fold increase in expression of Ngn1 which was easily observed by IHC (Figures. 2 D and 1 O, respectively). The rapid induction leads to a concurrent loss of stem cell markers and an increase in neural markers consistent with Ngn1 driving neural differentiation (Figures. 1, 2). The robust neural-inducing capacity of Ngn1 is consistent with several reports, not only in mES cells, but also in immortalized PC12 cells and mesechymal stem cells (Farah et al., 2000; Kim et al., 2008; Reyes et al., 2008). The specificity of Ngn1 is further supported by our data demonstrating a lack of endodermal or mesechymal differentiation (Figure. 1 S,T). These data confirm the robust induction properties of Ngn1 on mES cells as an exogenously inducible system.

We next wanted to characterize the maturation potential of neural progenitors generated by Ngn1 induction of N7 cells. We investigated the plasticity of N7 cells and their ability to respond to secondary signals and mature independently of the action of Ngn1. To do this, Ngn1-induced N7 cells were subjected to a standard motor neuron differentiation assay (Wichterle and Peljto, 2008). Ngn1 expression was long lasting, persisting beyond the 7 d motor neuron differentiation protocol without any further Dox treatment (Figure. 3 A). N7 cells that in which Ngn1 had been induced showed clear increases in the number of neural progenitors present in EBs (nestin, Figure. 3 B) and an increase in the number of mature neurons (represented by GluR2, Figure. 4 F) as previously demonstrated by Reyes *et.al* (Reyes et al., 2008). The presence of an increased number of mature neurons is also

represented in the number of motor neurons in the EBs. N7 cells expressing to Ngn1 prior to motor neuron patterning showed similar numbers of Olig2-expressing cells and higher numbers of Islet 1/2-positive cells (Figure. 3 F, Figure. 4 D), suggesting that the combination of Ngn1 and patterning molecules results in a higher number of mature cells. During normal maturation of the spinal cord, concurrent expression of multiple transcription factors establishes domains that give rise to specific neuronal subtypes (Shirasaki and Pfaff, 2002). Ngn1 has a biphasic action in tissue specification and differentiation; initially, Ngn1 specifies an early neuronal phenotype which can be further specified by growth factors and the microenvironment (Novitch et al., 2001; Zhou et al., 2001), suggesting that sustained Ngn1 expression may limit the later differentiation potential of N7 cells. Our data indicate, however, that EBs exposed to maintained Ngn1 expression are capable of producing motor neuronal subtypes (Figures. 3, 4). This data suggests that our Ngn1 induction paradigm is sufficient to generate neural progenitors from mES cells without limiting their differentiation potential despite prolonged Ngn1 expression. Furthermore, modification of this approach using different or multiple transcription factors could provide alternative lineage specifications for adaptation to various conditions (Hester et al., 2011).

Once we established the extent of neural induction in N7 cells *in vitro*, we next examined differentiation and maturation potential of N7 cells *in vivo*. First we examined if systemic Dox treatment was sufficient to drive neural induction of N7 cells grafted into the rat spinal cord. Administration of Dox to the rats via drinking water did not induce complete neural differentiation or stop proliferation of N7 cells, resulting in poor health and tumor formation (Figure. 5 A) despite the fact that systemic Dox penetrates the blood brain barrier (Lindeberg et al., 2002). Our *in vitro* data demonstrates that 3 d of Dox was sufficient to prime the cells towards a neural phenotype with a decreasing proliferative profile (Figure. 2). Therefore, we utilized primed N7 cells with a decreased proliferative potential along with systemic Dox treatment to circumvent tumor formation. When we analyzed the spinal cords of animals grafted with primed N7 cells, we observed successful cell transplants without tumor formation (Figure. 5 B). These data suggest that priming mES cells to differentiate is essential to prevent proliferation and tumor formation.

To characterize the N7 cell grafts, we first analyzed the residual stem cell and proliferating cell populations within the spinal cord. There were very few Oct3/4-positive stem cells and Ki67-postive proliferating cells remaining in the graft at this point (Figure. 5 C,D,G–I). Indeed our paradigm has lower levels of residing stem cells than are present in the 4 week study by Reyse et .al. using the same cells (Reyes et al., 2008). Other stem cell grafting studies have also demonstrated low level residual proliferating cells that do not go on to become long-term complications (Xu et al., 2009; Xu et al., 2006; Yan et al., 2007). Indeed, the current study utilizes a very short graft paradigm in order to understand the initial differentiation and behavior of stem cells *in situ*; therefore, future studies of longer duration are necessary to establish if all proliferating cells are eliminated, or if there are residual populations of stem cells that may continue to proliferate. Next, we wanted to establish the differentiation potential of the neural progenitors derived from the grafted N7 cells. We assessed several transcription factors associated with dorsoventral patterning and we observed markers of all dorsoventral regions of the spinal cord (Figure.6 A–G). Expression of these markers was not observed in the contralateral side of the spinal cord (Figure. 6 A'–G'). These data suggest that N7 cells are maturing in response to patterning signals endogenously expressed within the spinal cord.

While Ngn1 is highly associated with the generation of neural lineages, it has been shown to inhibit gliogenseis (Reyes et al., 2008; Sugimori et al., 2007; Sun et al., 2001). We did not observe any GFAP-positive cells in the cell cultures, EBs, or spinal cord grafts (data not shown). For future application for disease models where inhibition of gliogenesis could be

beneficial, maintained Ngn1 expression may be warranted after implantation of primed N7 cells (Lasiene and Yamanaka, 2011; Sahni and Kessler, 2010).

CONCLUSIONS

In this present study, we have demonstrated that inducible expression of Ngn1 in mES cells is sufficient to drive neural induction. Moreover, when these cells are grafted into the spinal cord, they are capable of responding to endogenous signals and differentiate into spinal progenitor lineages of both interneurons and motor neuron/oligodendrocyte progenitors (Figure. 6 H). While this study was designed to understand the first steps of differentiation and determine if the cells were capable of responding to signals within the spinal cord, more long-term studies are needed to elucidate the terminal phenotype, longevity and integration of these cells. These experiments validate Ngn1 induction of stem cells as a potential mechanism to safely introduce stem cells into the spinal cord, and may provide a source of cellular therapy for spinal cord injury or neurodegenerative diseases such as ALS and SMA.

Highlights

- Neural progenitors are generated from N7 mES cells within 3 days of Ngn1 expression
- N7 neural progenitors may be patterned and matured along different neural lineages
- Ngn1-induced neural progenitors averts tumor formation after intraspinal injection
- Grafted Ngn1-induced N7 cells differentiate into spinal cord progenitor cells

Acknowledgments

This work was supported by the A. Alfred Taubman Medical Research Institute and the Program for Neurology Research and Discovery. S.O. is supported by NS-39438. C.P. is supported by the US-Israel Binational Science Foundation.

ABBREVEATIONS

EB	Embryoid Body
Dox	Doxycycline
mES	mouse embryonic stem
ES	Embryonic stem
Ngn1	Neurogenin 1
EdU	ethynyl-2’-deoxyuridine
RA	retinoic acid and
Shh	sonic hedgehog

REFERENCES

Cawthorne C, et al. Comparison of doxycycline delivery methods for Tet-inducible gene expression in a subcutaneous xenograft model. J Biomol Tech. 2007; 18:120–123. [PubMed: 17496224]

Chesnutt C, et al. Coordinate regulation of neural tube patterning and proliferation by TGFbeta and WNT activity. Dev Biol. 2004; 274:334–347. [PubMed: 15385163]

Chung S, et al. Genetic selection of sox1GFP-expressing neural precursors removes residual tumorigenic pluripotent stem cells and attenuates tumor formation after transplantation. J Neurochem. 2006; 97:1467–1480. [PubMed: 16696855]

Drukker M. Immunogenicity of embryonic stem cells and their progeny. Methods Enzymol. 2006; 420:391–409. [PubMed: 17161708]

Farah MH, et al. Generation of neurons by transient expression of neural bHLH proteins in mammalian cells. Development. 2000; 127:693–702. [PubMed: 10648228]

Goldring CE, et al. Assessing the safety of stem cell therapeutics. Cell Stem Cell. 2011; 8:618–628. [PubMed: 21624806]

Hefferan MP, et al. Optimization of immunosuppressive therapy for spinal grafting of human spinal stem cells in a rat model of ALS. Cell Transplant. 2011

Hentze H, et al. Teratoma formation by human embryonic stem cells: evaluation of essential parameters for future safety studies. Stem Cell Res. 2009; 2:198–210. [PubMed: 19393593]

Hester ME, et al. Rapid and Efficient Generation of Functional Motor Neurons From Human Pluripotent Stem Cells Using Gene Delivered Transcription Factor Codes. Mol Ther. 2011

Jung J, et al. Ablation of tumor-derived stem cells transplanted to the central nervous system by genetic modification of embryonic stem cells with a suicide gene. Hum Gene Ther. 2007; 18:1182–1192. [PubMed: 18021021]

Kelloff GH, Sigman CC. New science-based endpoints to accelerate oncology drug development. Eur.J Cancer. 2005; 41:491–501. [PubMed: 15737552]

Kim HS, et al. Identification of a family of low-affinity insulin-like growth factor binding proteins (IGFBPs): characterization of connective tissue growth factor as a member of the IGFBP superfamily. Proc Natl Acad Sci U S A. 1997; 94:12981–12986. [PubMed: 9371786]

Kim S, et al. Neurogenin1 is sufficient to induce neuronal differentiation of embryonal carcinoma P19 cells in the absence of retinoic acid. Cell Mol Neurobiol. 2004; 24:343–356. [PubMed: 15206818]

Kim SS, et al. Neural induction with neurogenin1 increases the therapeutic effects of mesenchymal stem cells in the ischemic brain. Stem Cells. 2008; 26:2217–2228. [PubMed: 18617687]

Kiuru M, et al. Genetic control of wayward pluripotent stem cells and their progeny after transplantation. Cell Stem Cell. 2009; 4:289–300. [PubMed: 19341619]

Lasiene J, Yamanaka K. Glial cells in amyotrophic lateral sclerosis. Neurol Res Int. 2011; 2011:718987. [PubMed: 21766027]

Lindeberg J, et al. Timing the doxycycline yields different patterns of genomic recombination in brain neurons with a new inducible Cre transgene. J Neurosci Res. 2002; 68:248–253. [PubMed: 11948670]

Lunn JS, et al. Stem cell technology for the study and treatment of motor neuron diseases. Regen Med. 2011; 6:201–213. [PubMed: 21391854]

Lunn JS, et al. Vascular endothelial growth factor prevents G93A-SOD1-induced motor neuron degeneration. Dev Neurobiol. 2009; 69:871–884. [PubMed: 19672955]

Morrison SJ. Neuronal differentiation: proneural genes inhibit gliogenesis. Curr Biol. 2001; 11:R349–R351. [PubMed: 11369245]

Nakada Y, et al. Separable enhancer sequences regulate the expression of the neural bHLH transcription factor neurogenin 1. Dev Biol. 2004; 271:479–487. [PubMed: 15223348]

Nishimoto KP, et al. Modification of human embryonic stem cell-derived dendritic cells with mRNA for efficient antigen presentation and enhanced potency. Regen Med. 2011; 6:303–318. [PubMed: 21548736]

Novitch BG, et al. Coordinate regulation of motor neuron subtype identity and pan-neuronal properties by the bHLH repressor Olig2. Neuron. 2001; 31:773–789. [PubMed: 11567616]

Payne N, et al. The prospect of stem cells as multi-faceted purveyors of immune modulation, repair and regeneration in multiple sclerosis. Curr Stem Cell Res Ther. 2011; 6:50–62. [PubMed: 20955155]

Quinones HI, et al. Neurogenin 1 (Neurog1) expression in the ventral neural tube is mediated by a distinct enhancer and preferentially marks ventral interneuron lineages. Dev Biol. 2010; 340:283–292. [PubMed: 20171205]

Reyes JH, et al. Glutamatergic neuronal differentiation of mouse embryonic stem cells after transient expression of neurogenin 1 and treatment with BDNF and GDNF: in vitro and in vivo studies. J Neurosci. 2008; 28:12622–12631. [PubMed: 19036956]

Sahni V, Kessler JA. Stem cell therapies for spinal cord injury. Nat Rev Neurol. 2010; 6:363–372. [PubMed: 20551948]

Shirasaki R, Pfaff SL. Transcriptional codes and the control of neuronal identity. Annu Rev Neurosci. 2002; 25:251–281. [PubMed: 12052910]

Sobani ZA, et al. Stem cells for spinal cord regeneration: Current status. Surg Neurol Int. 2010; 1:93. [PubMed: 21246060]

Sugimori M, et al. Combinatorial actions of patterning and HLH transcription factors in the spatiotemporal control of neurogenesis and gliogenesis in the developing spinal cord. Development. 2007; 134:1617–1629. [PubMed: 17344230]

Sun Y, et al. Neurogenin promotes neurogenesis and inhibits glial differentiation by independent mechanisms. Cell. 2001; 104:365–376. [PubMed: 11239394]

Tong M, et al. The intrinsic electrophysiological properties of neurons derived from mouse embryonic stem cells overexpressing neurogenin-1. Am J Physiol Cell Physiol. 2010; 299:C1335–C1344. [PubMed: 20861468]

velkey, JM. Cell and Developmental Biology. vol. Ph.D. University of Michigan: Ann Arbor; 2005. Lineage Differentiation of Embryonic stem cells.

Wichterle H, Peljto M. Differentiation of mouse embryonic stem cells to spinal motor neurons. Chapter 1. Curr Protoc Stem Cell Biol. 2008 Unit 1H 1 1-1H 1 9.

Xu L, et al. Human neural stem cell grafts in the spinal cord of SOD1 transgenic rats: differentiation and structural integration into the segmental motor circuitry. J Comp Neurol. 2009; 514:297–309. [PubMed: 19326469]

Xu L, et al. Human neural stem cell grafts ameliorate motor neuron disease in SOD-1 transgenic rats. Transplantation. 2006; 82:865–875. [PubMed: 17038899]

Yan J, et al. Extensive neuronal differentiation of human neural stem cell grafts in adult rat spinal cord. PLoS Med. 2007; 4:e39. [PubMed: 17298165]

Zhou Q, et al. The bHLH transcription factor Olig2 promotes oligodendrocyte differentiation in collaboration with Nkx2.2. Neuron. 2001; 31:791–807. [PubMed: 11567617]

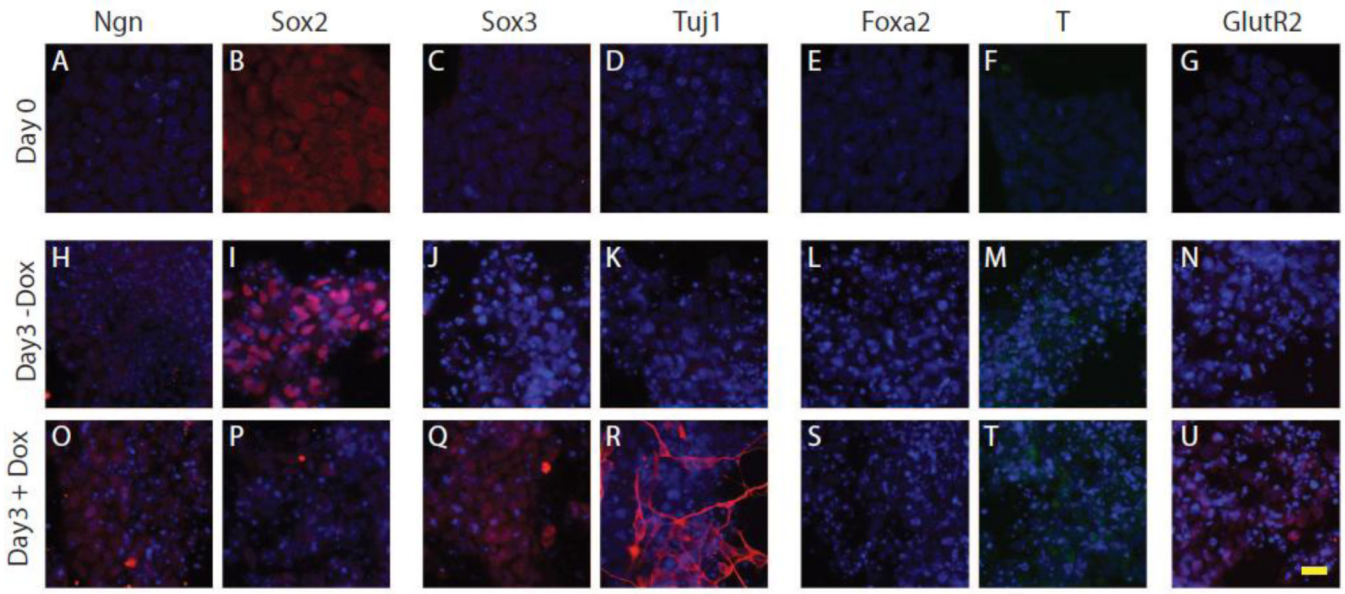

Figure 1. Ngn1-induced neural induction of N7 cells

A–G. Immunohistochemical staining for stem cell markers (Ngn A,H,O, and Sox2, B,I,P), pro-neural markers (Sox3, C,J,Q and Tuj1 D,K, R), endoderm (Foxa2 E, L, S), mesoderm (Brachyury F,M, T) and AMPA receptor (GluR2 G,N, U) in N7 cells under undifferentiated growth conditions. **H–U**. Cells were grown for 3 d in differentiation media with Dox (O–U) or without Dox (H–N). Scale bar 20 μm

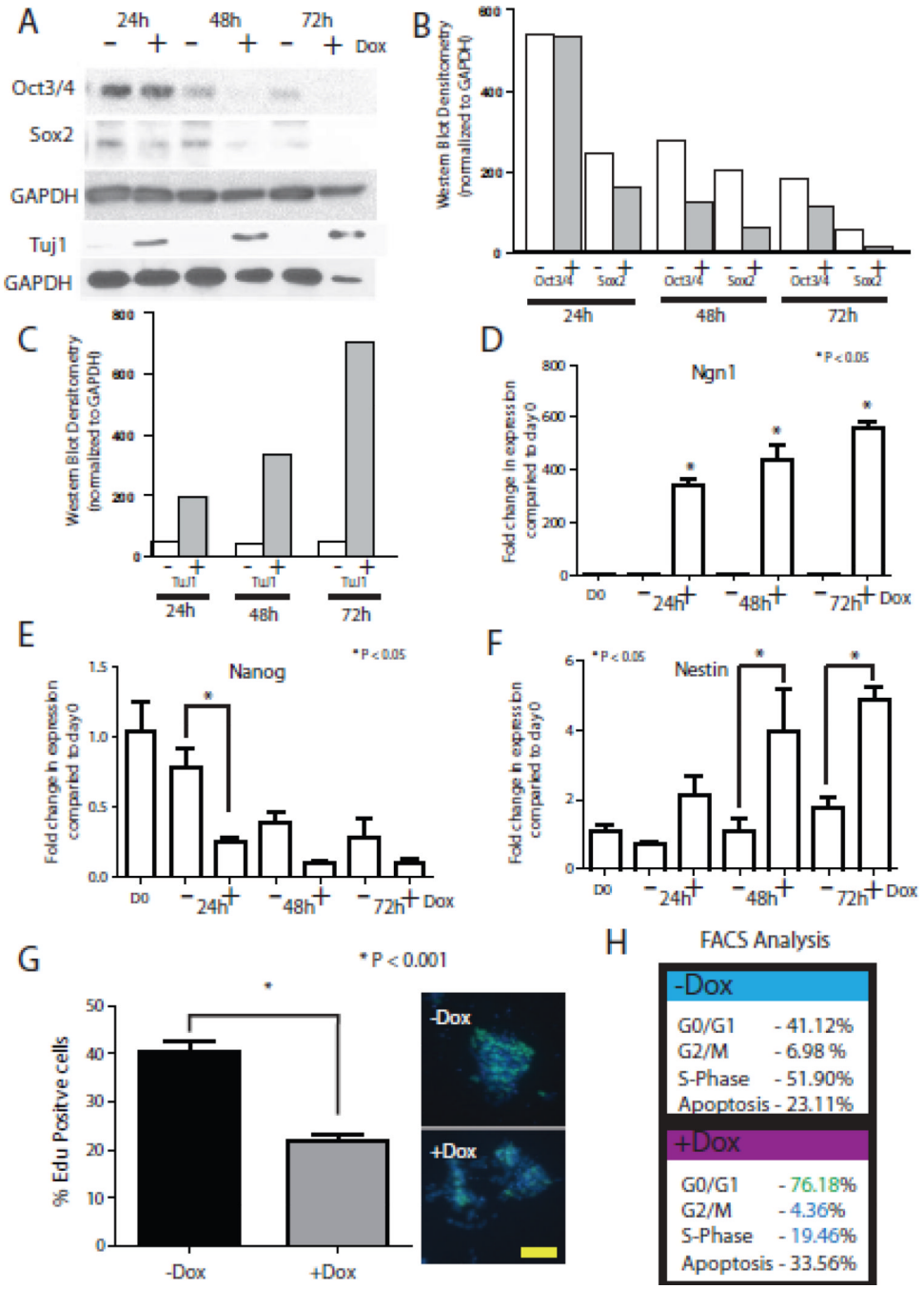

Figure 2. Quantification of Dox induction in N7 cells

A. Western blot analysis of N7 cells over 3 d of differentiation with or without Dox. Blot stained for stem cell markers (Oct3/4, Sox2), neural marker (TuJ1), and loading control (GAPDH). **B–C** Analysis of western blotting using densitometry, values equalized to GAPDH loading. **D–F**. QPCR analysis of N7 cell differentiation analyzing induction of Ngn1 (D), a stem cell marker Nanog (E), and the neural marker nestin (F). **G**. Representative images of EdU incorporation into proliferating N7 cells after 3 d differentiation with or without Dox. Scale bar 100 μm. **H**. FACS analysis of cell cycle stages and apoptosis at 3 d differentiation with or without Dox after staining with PI.

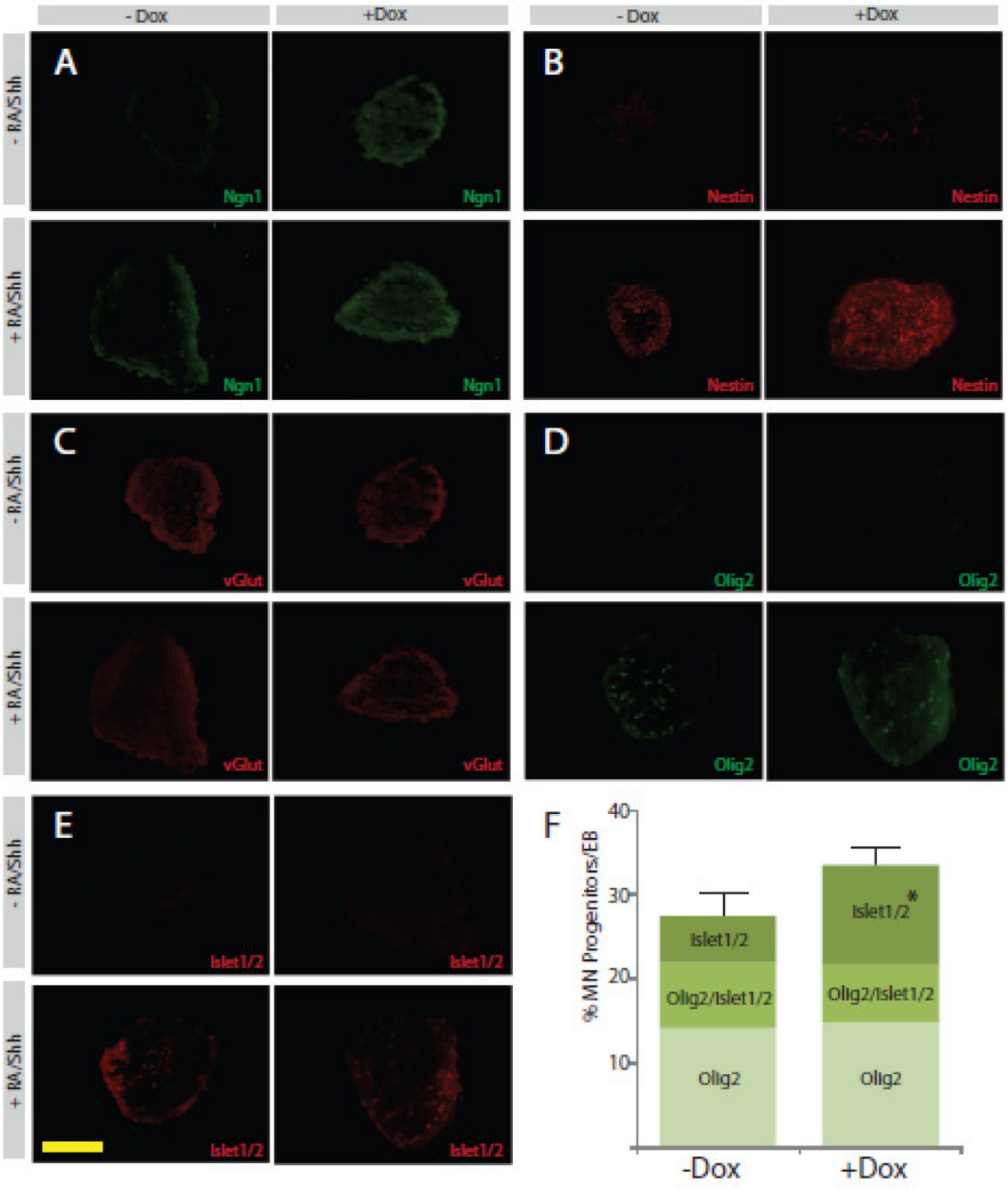

Figure 3. Patterning of N7 cells induced with Ngn1 by exogenous signaling factors

A–E. Four panel figures represent sections of EBs made from N7 cells grown for 3 d with or without Dox, followed by EBs grown with or without patterning with RA and shh. IHC for Ngn1 (A), nestin (B), vGlut (C), Olig2 (D) and Islet 1/2 (E). **F**. Quantification of cells stained positive for Olig2 alone, Olig2/Islet 1/2 or Islet1/2 alone, represented as a percent of the total cells per EB. Scale bar 50 μm

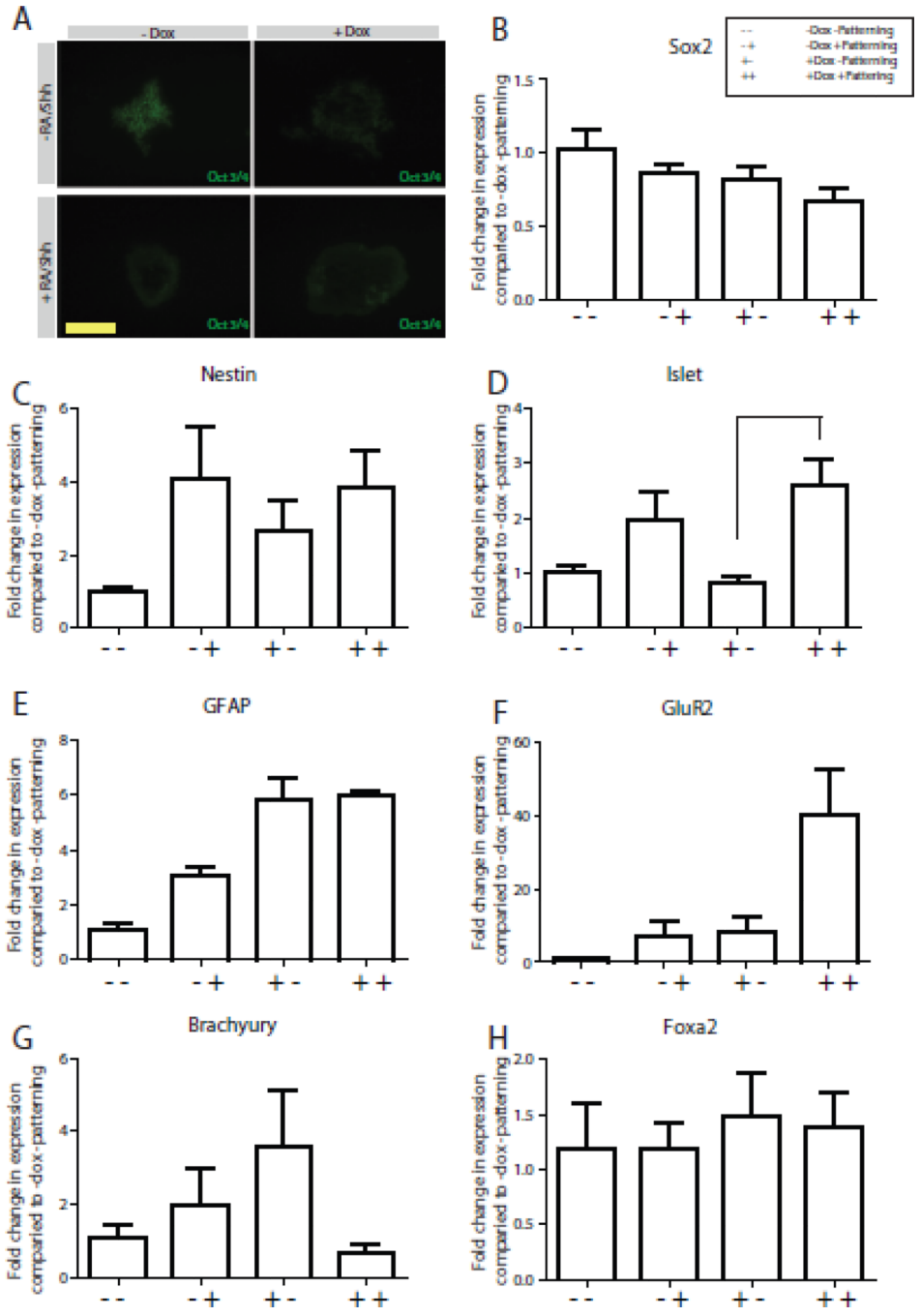

Figure 4. Quantification of EB identity following MN differentiation

A. Four panel figures represent sections of EBs made from N7 cells grown for 3 d with or without Dox, followed by EBs grown with or without patterning with RA and shh stained for Oct3/4 expression. Scale bar 50 μm. **B–H**. QPCR of EBs made from N7 +/−Dox, +/− RA/Shh patterning for Sox2 (B), Nestin (C), Islet1/2 (D), GFAP (E), GluR1 (F), Brachyury (G) and Foxa2 (H).

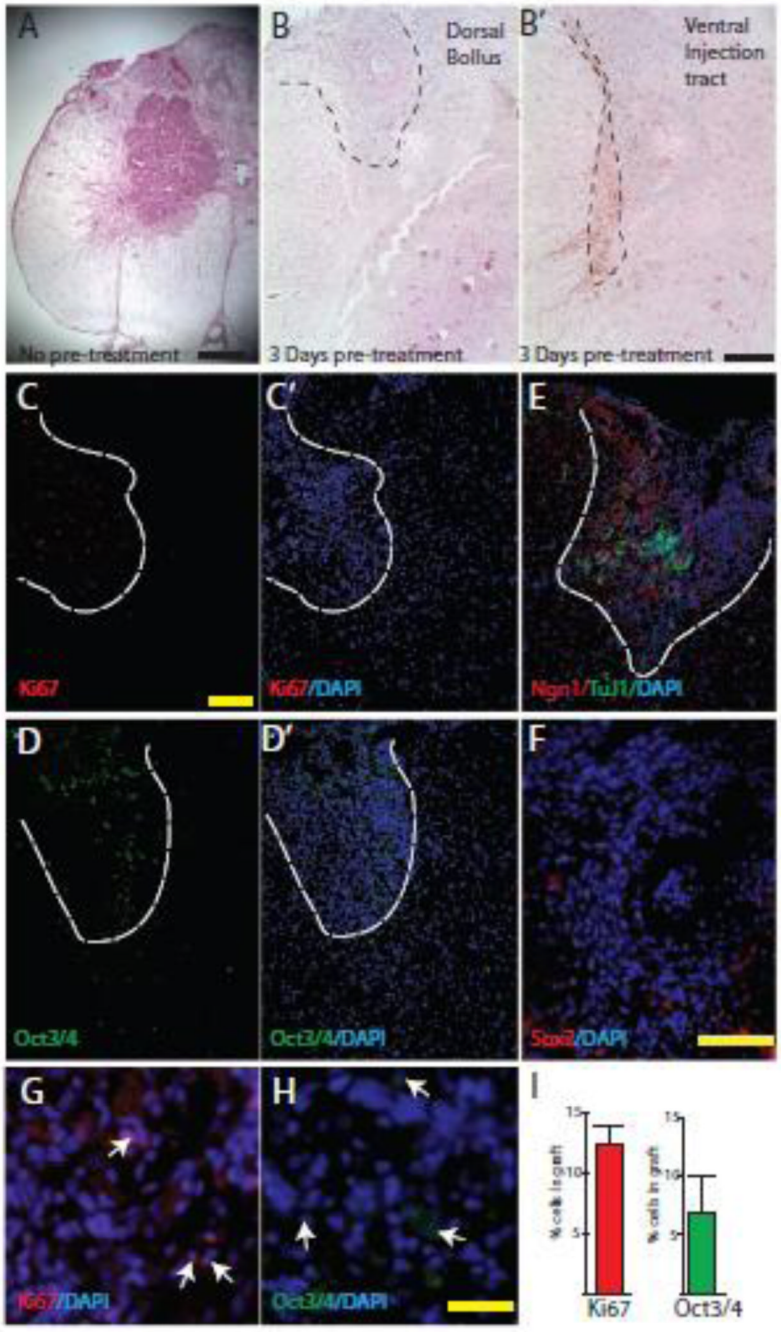

Figure 5. Examination of stem cell phenotype after spinal implantation of N7 cells

Spinal cord cross sections from animals after intraspinal injection of N7 mES cells **A–B**. H&E staining of spinal cords without Dox pretreatment of N7 cells (A) or with Dox pretreatment (B). Scale bar 400 μm (A), 200 μm (B'). **C–H**. IHC staining of spinal cord cross sections injected with primed N7 cells for proliferation marker Ki67 (C; inset shows number of Ki67 cells per graft) and stem cell marker Oct 3/4 (D; inset shows number of Oct3/4 cells per graft) Scale bar 200 μm. **G,H** Higher power image of Ki67 and Oct3/4 staining, positive cells labeled with white arrows, scale bar 50 μm. **E.** Double labeling Ngn1

(red) and, Tuj1 (green) to identify graft area. **F.** No Sox2 positive cells within the graft area, but some in host tissue, scale bar 100 μm.

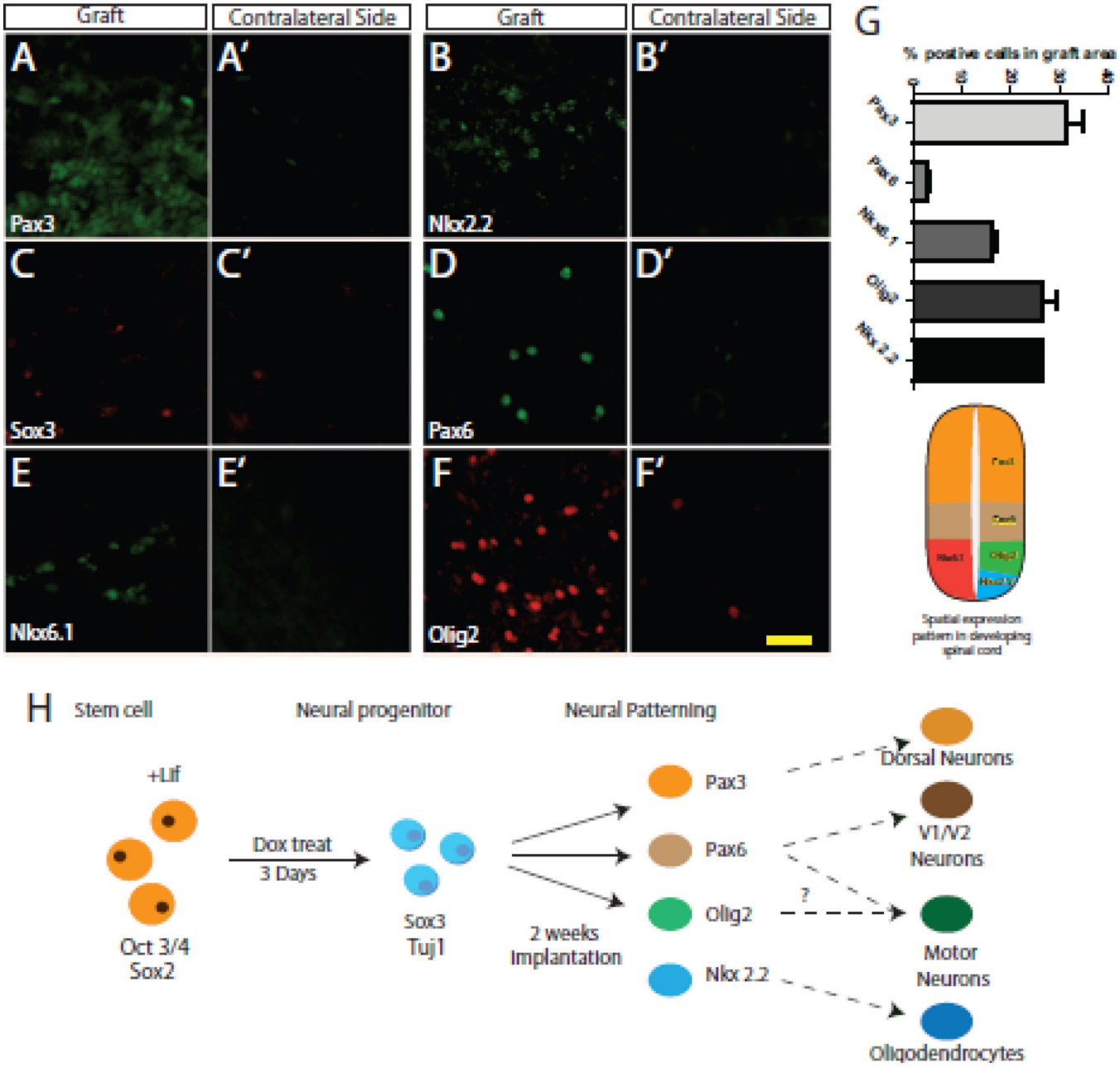

Figure 6. Differentiation of N7 cells in the spinal cord

A–F. Representative images of IHC for Pax3 (A), Nkx2.2 (B), Sox2 (C), PAx6 (D), Nkx6.1 (E) and Olig2 (F) in the graft area of the spinal cord. **A'–F'** Representative images taken from the contralateral side of the spinal cord. **G**. Quantification of expression in the graft area, graph aligned with an illustration of the dorsoventral patterning of the spinal cord. **H**. Model demonstrating the differentiation of N7 cells through the course of the experiments. Scale bar 100 μm

Table 1

QPCR Primers

Gene	Forward	Reverse
Brachyury	CGGATTCACATCGTGAGAGTT	AGGCTTTAGCAAATGGGTTGT
Foxa2	GGCCAGCGAGTTAAAGTATGC	CATGTTGCTCACGGAAGAGTAG
GFAP	TGCAAGAGACAGAGGAGTGGT	GCGATAGTCGTTAGCTTCGTG
GluR1	CACAGTGAAGAGTTTGAAGAAGGA	TAATCAAAGTGAAGAACCACCAGA
Islet1/2	ACCAGTATATTCTGAGGGTTTCTC	TTGATCCCGTACAACCTGATATAAT
Nanog	CTCCATTCTGAACCTGAGCTATAA	AATCAGACCATTGCTAGTCTTCAA
Nestin	TGCAGACACCTGGAAGAAGTT	TATTAGGCAAGGGGGAAGAGA
Neurogenin1	ACCACTCTCTGACCCCAGTAGTC	GTCGTGTGGAGCAGGTCTTT
Olig2	CTGGTGTCTAGTCGCCCATC	GACACAGTCCCTCCTGTGAAG
Sox2	CACCTACAGCATGTCCTACTC	AGTGGGAGGAAGAGGTAACCA